Tribology and Materials
Vol. 4, No. 1, 2025, pp. 18-28

ISSN 2812-9717
https://doi.org/10.46793/tribomat.2025.002

Boron nitride nanosheets and silica nanoparticles reinforced polypropylene: Rheological, thermal, mechanical and tribological behaviour

Narava Divya APARNA, Pankaj TAMBE*

School of Mechanical Engineering, VIT-AP University, Amravati, India
*Corresponding author: pankaj.tambe@vitap.ac.in

Keywords
polypropylene
hybrid fillers
silica nanoparticles
nanocomposites
h-BN nanosheets

History
Received: 22-11-2024
Revised: 31-01-2025
Accepted: 06-02-2025

Abstract

In recent years, there has been increased attention to incorporating hybrid filler in polymer matrices to enhance the properties for various applications. In this work, hybrid fillers of hexagonal boron nitride (h-BN) nanosheets and silica (SiO_2) nanoparticles are incorporated in a polypropylene (PP) matrix using the melt mixing method. This study is focused on the rheological, thermal, mechanical and tribological behaviour of hybrid filler-reinforced PP-based nanocomposites. The incorporation of hybrid filler in the PP matrix shows an increase in viscosity compared to individual filler-reinforced PP due to the finer dispersion of hybrid filler in the PP matrix. The degree of crystallinity, tensile properties and thermal stability are the highest for the hybrid filler-reinforced PP-based nanocomposite. The increase in tensile modulus and tensile strength are 25 and 1 %, respectively. The wear is the lowest for the hybrid filler-reinforced PP-based nanocomposite.

1. Introduction

Polypropylene (PP) is a mass-produced thermoplastic widely used in industry [1-6]. Thus, PP is an attractive choice as a matrix material for composites. Additionally, PP can be easily recycled by melt compounding [7]. In the literature, PP is reinforced with many types of fillers to improve processability and tailor the properties for many applications. The filler materials added to the PP matrix were carbon black, halloysite nanotubes, carbon nanotubes, graphene, etc. [3-6]. The addition of these filler materials in PP revealed an improvement in mechanical properties. These filler material selections depended on the intended application's property requirements and cost considerations. In recent years, the use of hybrid fillers in polymer matrices has been a focus of research in the scientific community. The advantage of using hybrid fillers is that the different filler materials have various properties and shapes.

Hexagonal boron nitride (h-BN) nanosheets were used by many researchers as reinforcement in polymer matrices [8-10]. The main advantage of using h-BN nanosheets as a reinforcing material is their high modulus of elasticity and layered structure with lubricating properties. Kong et al. [11] modified the h-BN nanosheets with alkyl grafting, and their incorporation in the PP matrix increased the modulus of elasticity by 17 %. Muratov et al. [12] showed a 29 % increase in thermal conductivity by incorporation of h-BN nanosheets in the PP matrix.

Many researchers have studied silica (SiO_2) nanoparticles as reinforcement for polymer matrices [13-15]. Silica, being spherical in shape and high in hardness, is attractive for researchers as a reinforcing filler due to its low cost and availability. García et al. [15] have incorporated 4.5 wt. % silica in a PP matrix, resulting in a 33 % enhancement in modulus of elasticity. Palza et al. [16] have shown that spherical silica is a better-reinforcing filler for PP than layered silica.

Many researchers also studied the hybrid filler-reinforced PP-based composites. Sinha et al. [8] used

graphene and titanium dioxide as a hybrid filler in a PP matrix to improve the mechanical properties. Graphene was the most significant parameter, followed by titanium dioxide, for enhancing the PP properties. Kufel et al. [17] used basalt and glass fibre in a PP matrix to improve tensile strength and tensile modulus by 306 and 333 %, respectively. Nurdina et al. [18] studied the combination of calcium carbonate, mica and silica in a PP matrix, which improved tensile modulus by 38 % when 40 vol. % filler was added. Hartikainen et al. [19] studied the orientation effect and fracture behaviour of glass fibre and calcium carbonate particulate filler-reinforced PP-based composites. Hayajneh et al. [20] used eggshell and lemon leaves as a filler in PP to improve the tensile modulus by 23 % when 10 wt. % filler was added. Watt et al. [21] processed biocarbon and graphene nanoplatelet-reinforced PP-based nanocomposites for mechanical and thermal properties enhancement. Biocarbon uniform dispersion, resisting graphene from aggregates in the PP matrix, was responsible for the enhancement of mechanical properties.

In this work, hexagonal boron nitride (h-BN) nanosheets and silica (SiO_2) nanoparticles are used as hybrid nanofillers. The h-BN nanosheets are lubricating materials and their dispersion in the PP matrix can influence the tribological properties. On the other hand, silica is a hard material and its incorporation in the PP matrix can influence the mechanical properties. Thus, the hybrid filler was incorporated into the PP matrix and studied for its influence on the mechanical, thermal, rheological and tribological behaviour. In addition, polypropylene grafted maleic anhydride (PP-G-MA) was used. The melt mixing method for processing nanocomposites was used since it is of industrial importance.

2. Experimentation

2.1 Materials

The micron-size h-BN powder was procured from Momentive Performance Materials, India. It has a mean particle size of 5 µm and a specific surface area of 30 m^2/g. Silica nanoparticles were procured from Fiber Region, India and had an average diameter of 70 nm. PP (Repol H110MA) was procured from Reliance Industries, India having a melt flow rate of 11 g/10 min at 2.16 kg and 230 °C. The compatibilizer (PP-G-MA) with a melt flow rate of 15 g/10 min at 2.16 kg and 230 °C was procured from Plus Polymer, India.

2.2 Processing

The h-BN nanosheets were processed using the following procedure. The 3 g of h-BN powder was heated in a tube furnace at 1000 °C for 1 hour in an air atmosphere. Upon cooling, the powder was mixed with 750 ml of deionised water under continuous stirring on a magnetic stirrer for 1 hour. Further, sonication was done for 2 hours. Thereafter, the solution was centrifuged and washed repeatedly with distilled water to reach a pH 7 value. The washed h-BN nanosheets were dried in a vacuum oven at 80 °C for 6 hours to obtain h-BN nanosheets.

The neat PP and PP-based nanocomposites have been processed using a twin screw extruder followed by pelletization. The extruder was operated in temperature zones of 165 – 210 – 230 °C, with exit nozzle temperature maintained at 230 °C and screw speed of 90 rpm. The injection moulded was done with a pressure of 1 MPa, which was used to push the material inside the die cavity to obtain the test specimens. The injection moulding die was maintained at 230 °C. The obtained sample from injection moulding was as per ASTM D638, Type IV. The PP and PP-based nanocomposites were vacuum-dried at 80 °C.

The concentration of silica nanoparticles, h-BN nanosheets and their hybrid was 1 wt. %. The ratio of hybrid filler SiO_2:h-BN was 1:1, which means 0.5 wt. % h-BN nanosheets and 0.5 wt. % SiO_2 nanoparticles dispersed in the PP matrix. The material designation is done based on the composition (PP is polypropylene, GM is PP-G-MA, Si is silica nanoparticles and hBN is h-BN nanosheets) as follows: PP for neat PP sample, PPGMSi for PP/Si nanocomposite, PPGMhBN for PP/hBN nanocomposite and PPGMhBNSi for PP/Si/hBN nanocomposite.

2.3 Characterisation

The h-BN nanosheets were characterised using X-ray diffraction (XRD) and transmission electron microscopy (TEM). The XRD was done with a Malvern Panalytical Empyrean diffractometer, using Cu Kα radiation with a wavelength of 1.54 Å and a scanning range of 5 – 90°. The TEM was done with a FEI Tecnai G^2 F30 transmission electron microscope.

Scanning electron microscopy (SEM) was done on silica nanoparticles with a Carl Zeiss Supra 55 scanning electron microscope. Cryofracture of PP-based nanocomposites was done to have a brittle

fracture and locate the nanoparticles dispersed in the matrix by SEM. In addition, XRD and SEM of PP and PP-based nanocomposites were done.

Rheological characterisation was performed with an Anton Parr MCR 102 modular compact rheometer in a steady-state shear mode at 230 °C with a shear rate of 0.1 – 100 s^{-1}.

Differential scanning calorimetry (DSC) studies were done on a PerkinElmer STA 8000 thermal analyser. For a 5 to 15 mg sample, a heating-cooling-heating cycle was performed in a range of 30 – 230 °C at 10 °C/min under a nitrogen atmosphere. The degree of crystallinity was obtained from the ratio of the melting enthalpy of the sample and the melting enthalpy of 100 % crystalline PP, i.e. 207 J/g [3,4]. The thermogravimetric analysis (TGA) studies were done on PerkinElmer STA 8000 thermal analyser, in the heating cycle range of 30 – 900 °C at 20 °C/min in a nitrogen atmosphere. Two samples were tested for each material during DSC and TGA studies.

Tensile testing was done as per ASTM D638 using a Tinius Olsen H10KL universal testing machine at a crosshead speed of 5 mm/min. Five samples were tested for each material during tensile testing.

Tribological studies were done using a Ducom TR-20LE pin-on-disc tribometer at a disc speed of 200 rpm, applied normal load of 40 N and time of 1 hour. Pins were square samples of 10 × 10 mm and 4 mm thickness. Counter-body (disc) material was EN31 steel alloy, having a hardness of 65 HRC. The calculated sliding speed was 1.2 m/s. Friction force and thickness of worn material (wear thickness) were measured continuously with time. Three samples were tested for each material during tribological testing.

3. Results and discussion

3.1 Filler characterisation

Figure 1a shows the TEM image of h-BN nanosheets. It shows the h-BN nanosheets of varying sizes, between 100 – 500 nm. XRD was done to characterise the crystal structure of h-BN nanosheets (Fig. 1b). A sharp peak at 26.7° for (002) is seen in XRD spectra, confirming the hexagonal structure of h-BN nanosheets. Additionally, a peak at 41.8, 55 and 75.8°, which corresponds to (100), (004) and (110) planes of h-BN nanosheets, respectively, were noticed [22]. Figure 2 shows the SEM image of silica nanoparticles. The silica nanoparticles were spherical.

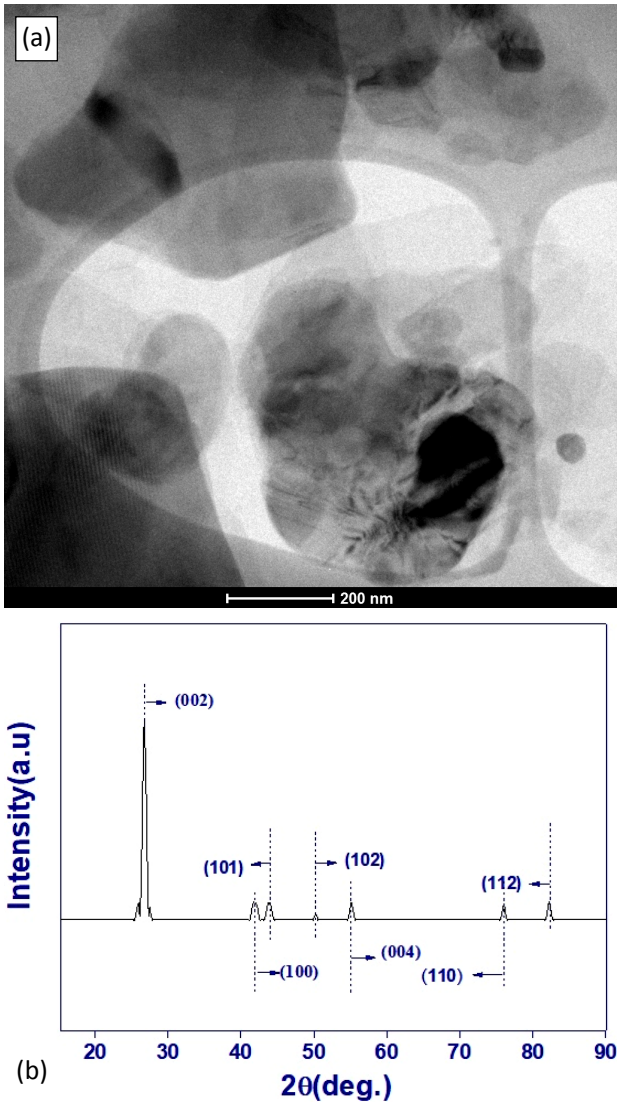

Figure 1. Characterisation of h-BN nanosheets: (a) TEM image and (b) XRD spectra

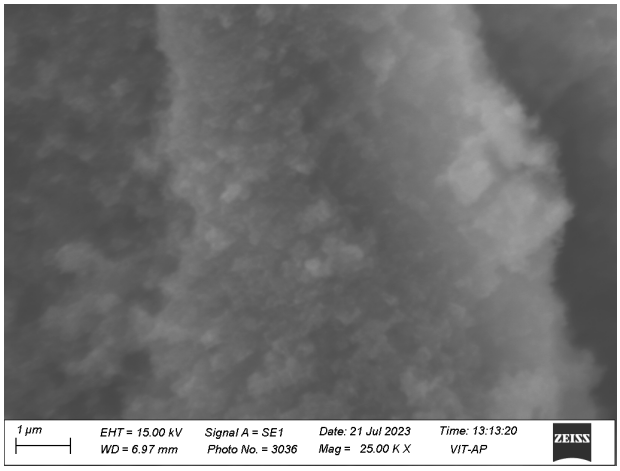

Figure 2. SEM image of spherical shape silica nanoparticles

3.2 Rheological characterisation

To understand the influence of filler addition on PP matrix flow behaviour, rheological studies were

done on PP and PP/hBN, PP/Si and PP/hBNSi nanocomposites. Figure 3 is a plot of steady-state rotational viscosity vs. shear rate of tested materials. From the viscosity curve of PP and PP-based nanocomposites, it could be noticed that they exhibit Newtonian behaviour at low shear rates. A shear thinning region is noticed at higher shear rates, depicting a decrease in viscosity.

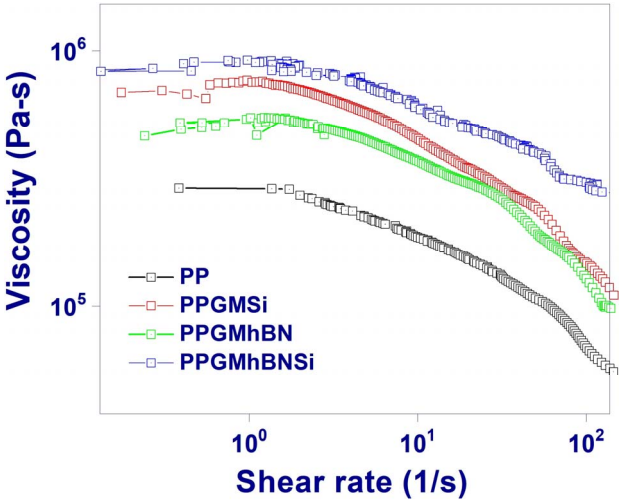

Figure 3. Steady-state rheology of PP and PP-based nanocomposites

The addition of 1 wt. % of silica in the PP matrix shows an increase in viscosity in the Newtonian plateau and shear thinning region. Since silica nanoparticles possess a high surface area, their dispersion in the PP matrix enhances the flow resistance of PP chains. For a PP/hBN nanocomposite, the viscosity values in the Newtonian plateau and shear thinning region are lower than those of the PP/Si nanocomposite but higher than those of the neat PP. As h-BN has a layered structure, the slip of the h-BN nanosheets in the PP matrix under rotational shear contributes to the noticed decrease in viscosity values in comparison with PP/Si nanocomposite. It is noticed that the viscosity curve of PP/hBNSi nanocomposite shows the highest increase in viscosity in the Newtonian plateau and shear thinning region. The possible reason is that the concentration of h-BN nanosheets is lower in the PP matrix and along with better dispersion of silica in the PP matrix, it facilitates the restriction of slip of h-BN nanosheets and PP chains [22].

To understand the relationship between the deformation of the polymer chains and their resistance to flow under stress, the power-law model can be fitted. The power-law model was applied to understand the flow behaviour of PP and PP-based nanocomposites. The power-law model is written as follows [23].

$$\eta = K\gamma^{n-1}, \quad (1)$$

where η is apparent viscosity in Pas, K is flow consistency index in Pas^n, γ is shear rate in s^{-1} and n is flow behaviour index.

The power-law model shows a direct relationship between viscosity and shear rate. The constants in the equation n and K can be determined by analysing the slope and intercept of the data, respectively.

Table 1 presents calculated flow behaviour index (n) and apparent viscosity (η) for each material at a specific shear rate. All materials exhibit a flow behaviour index of less than 1, indicating that they behave as pseudoplastic fluids. The PP shows a viscosity of 1.8×10^5 Pas at a shear rate of 10 s^{-1}, with n value of 0.61. The addition of silica in the PP matrix induces a decrease in n value to 0.55, with the viscosity value increasing to 4.4×10^5 Pas at the same shear rate. The decreased n value for PP/Si nanocomposite indicates an improvement in processability. Introducing 1 wt. % h-BN in the PP matrix results in a decreased n value to 0.6, and a viscosity value increased to 3.4×10^5 Pas at the shear rate of 10 s^{-1}, also indicating improved processability. Furthermore, the addition of h-BN and silica to PP increased the n value to 0.74 and viscosity to 5.9×10^5 Pas at a shear rate of 10 s^{-1}. The increase in n value depicts the synergistic effect of hybrid filler components in reducing the PP chain mobility. The increased viscosity can be used as a measure of the dispersion state of hybrid filler in the polymer matrix.

Table 1. Flow behaviour index and apparent viscosity of PP and PP-based nanocomposites

Material	Apparent viscosity at 1 s^{-1}, Pas	Apparent viscosity at 10 s^{-1}, Pas	Flow behaviour index
PP	1.0×10^5	1.8×10^5	0.61
PPGMSi	7.3×10^5	4.4×10^5	0.55
PPGMhBN	5.4×10^5	3.4×10^5	0.60
PPGMhBNSi	9.2×10^5	5.9×10^5	0.74

3.3 SEM characterisation of cryofractured samples

Figure 4 shows the SEM images of cryofractured PP/hBN and PP/hBN/Si nanocomposites. Figure 4a shows the fibril formation due to the localised deformation of PP chains in the presence of h-BN

nanosheets. Sharp and curved fibril edges reveal the presence of h-BN nanosheets in the PP matrix. Figure 4b shows the PP/hBN/Si nanocomposite and the presence of encircled spherical silica with parallel edges, revealing the presence of the h-BN nanosheets.

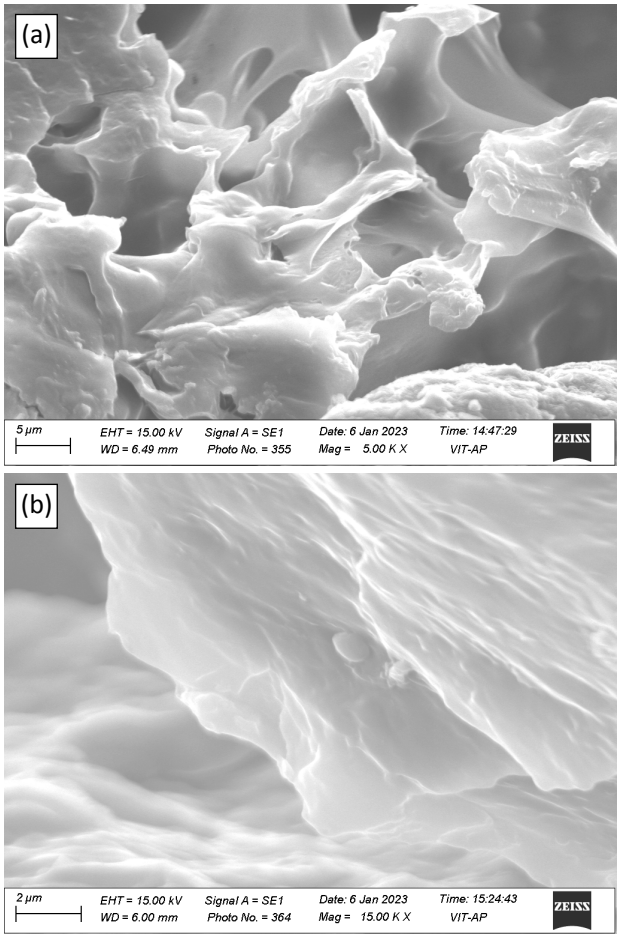

Figure 4. SEM images of cryofractured nanocomposites: (a) PP/hBN and (b) PP/hBN/Si

3.4 XRD characterisation

Figure 5 shows the XRD spectra of PP and PP-based nanocomposites. The XRD spectra of PP shows five peaks at 2θ equal to 13.86, 16.68, 18.27, 21.55 and 25.21°. This is corresponding to (110), (040), (130), (131) and (060) crystallographic planes of the α-crystal form of PP. In addition, a β-crystal form (300) plane at 2θ = 15.7° is noticed for PP. The addition of silica in PP shows that the XRD spectra have the α-crystal form of PP. Similarly, the addition of h-BN nanosheets in PP shows that the XRD spectra have the α-crystal form of PP. However, the intensity of the (040) peak is higher than the (110) peak, confirming the h-BN facilitates the formation of PP crystal along the (040) plane. An additional peak at 2θ = 26.6° for the (002) crystallographic plane of h-BN nanosheets is observed in XRD spectra of PP/hBN and PP/hBN/Si nanocomposites. This confirms the presence of multilayer h-BN nanosheets in the PP matrix.

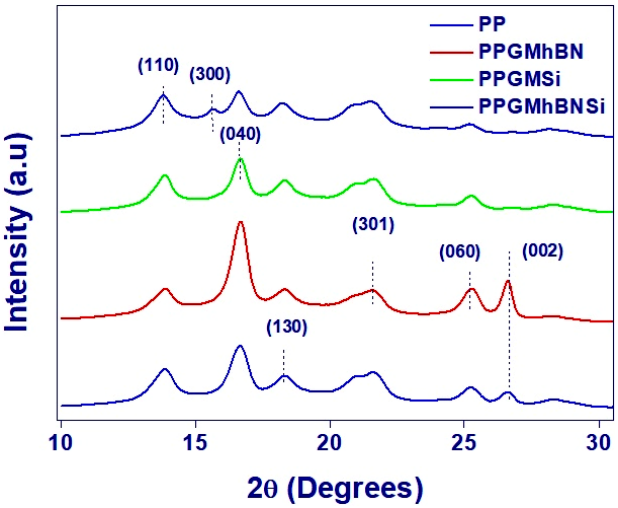

Figure 5. XRD spectra of PP and PP-based nanocomposites

3.5 DSC characterisation

DSC analysis was carried out over the PP and PP-based nanocomposites. Table 2 shows the quantified data from the DSC analysis.

Table 2. Crystallisation, melting and degree of crystallinity of PP and PP-based nanocomposites

Material	T_m, °C	T_{onset}, °C	T_c, °C	T_{diff}, °C	X_c, %
PP	168.2	125.3	114.5	10.8	37.8
PPGMSi	170.1	133.6	124.6	9.0	39.7
PPGMhBN	168.7	134.7	125.8	8.9	36.6
PPGMhBNSi	168.9	136.3	125.6	10.7	38.6

T_m – melting temperature; T_{onset} – onset temperature; T_c – crystallisation temperature; T_{diff} – difference in onset and crystalline temperature; X_c – degree of crystallinity

Figure 6a shows the crystallisation exotherms of PP and PP-based nanocomposites. The crystallisation exotherms show a single peak of PP. The crystallisation temperature (T_c) of PP is 114.6 °C. The addition of individual or hybrid filler in the PP matrix shows an increase in T_c. The increase in T_c is due to the heterogeneous nucleation effect of fillers on PP crystal formation. The T_c of PP/Si nanocomposite is lower than that of of PP/hBN nanocomposite. This reveals higher a surface area of contact of the h-BN nanosheet with the PP matrix in comparison with the silica and PP matrix. The T_c of the PP/hBNSi nanocomposite lies between the PP/Si and

PP/hBN nanocomposites, confirming the synergistic influence of hybrid filler components in dispersion.

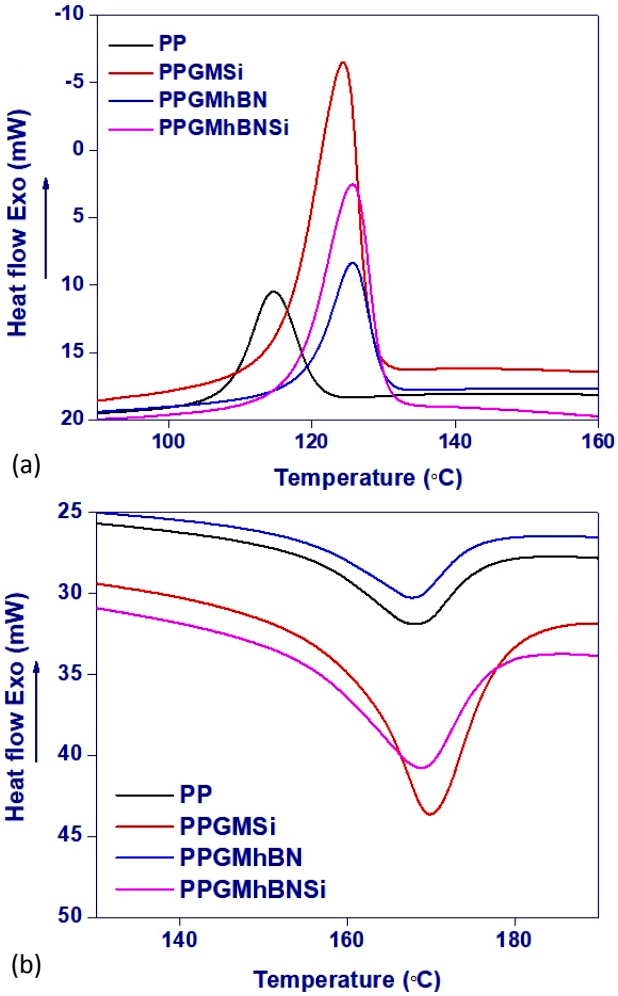

Figure 6. DSC analysis of PP and PP-based nanocomposites: (a) crystallisation exotherms and (b) melting endotherms

Figure 6b shows the melting endotherms of PP and PP-based nanocomposites. All melting endotherms show a single melting peak. The melting temperature (T_m) of PP is 168.2 °C. The T_m of PP/Si nanocomposite is 170.1 °C, which is higher than PP, depicting the aggregated dispersion of silica in the PP matrix. The T_m of PP/hBN nanocomposite is 168.7 °C, depicting the improved dispersion of h-BN nanosheets in the PP matrix and the higher surface area of contact between the PP and h-BN nanosheets. The T_m of PP/hBN/Si nanocomposite is 168.9 °C, which is higher than the PP but less than the PP/Si nanocomposite, depicting the synergistic effect of hybrid filler components in dispersion on the T_m of PP/hBN/Si nanocomposite.

The degree of crystallinity (X_c) of PP, PP/Si, PP/hBN and PP/hBN/Si nanocomposites are obtained using the DSC characterisation. It was calculated from the enthalpy values of the melting endotherm. The X_c of PP/Si nanocomposite is higher than the X_c of PP since silica acts as a heterogeneous nucleating agent. In addition, the difference in onset and crystalline temperature (T_{diff}) is smaller, confirming the influence on spherulitic morphology. The X_c decreases for PP/hBN nanocomposite because of the better dispersion of h-BN in the PP matrix, facilitating a more amorphous chain at the interphase. The X_c increase for PP/hBN/Si nanocomposite is due to the synergistic effect of hybrid filler components on the PP matrix. In the case of PP/hBN/Si nanocomposite, the concentration of h-BN in the matrix is lower, facilitating lower amorphous chain adsorption on the h-BN nanosheet surface. In addition, silica dispersion contributes significantly to the increase in crystallinity of PP.

3.6 TGA characterisation

Figure 7 shows thermogravimetric analysis (TGA) studies of the PP and PP-based nanocomposites. Figure 7a shows the TGA curves of PP and PP-based nanocomposites. The TGA curves of PP and PP-based nanocomposites show single-step degradation in the range of 340 – 510 °C. Figure 7b shows the differential thermogravimetric analysis (DTGA) curves of PP and PP-based nanocomposites. The thermal degradation temperature (T_d) of PP is 451.1 °C. The addition of silica in the PP matrix induces enhancement in T_d value to 452.5 °C. This suggests the influence of silica in improving the thermal stability of PP. Further, the T_d value of 453.2 °C for PP/hBN nanocomposite suggests that the addition of h-BN in the PP matrix also increases the thermal stability. The T_d value of 450.5 °C for PP/Si/hBN nanocomposite is lower than for PP, depicting no influence on thermal stability.

3.7 Tensile characterisation

Tensile testing was done on PP and PP-based nanocomposites. The stress-strain curves of PP and PP-based nanocomposites are shown in Figure 8a. The tensile strengths are shown in Figure 8b and calculated tensile modulus values are shown in Figure 8c. From the histogram of tensile modulus and tensile strength, it could be noticed that, compared to PP, values for PP containing h-BN nanosheets or silica nanoparticles were lower, while for PP/Si/hBN nanocomposite values were

increased, confirming the synergistic effect of hybrid filler components. The tensile modulus of PP is 2.41 GPa. The addition of silica in the PP matrix decreased the tensile strength by 3 % and tensile modulus by 7.9 % in comparison to PP. Further, adding h-BN nanosheets in the PP matrix decreased the tensile strength by 9.6 % and tensile modulus by 0.8 % compared to PP. Adding h-BN nanosheets and silica nanoparticles in the PP matrix increases the tensile strength by 1 % and tensile modulus by 21.5 % compared to PP.

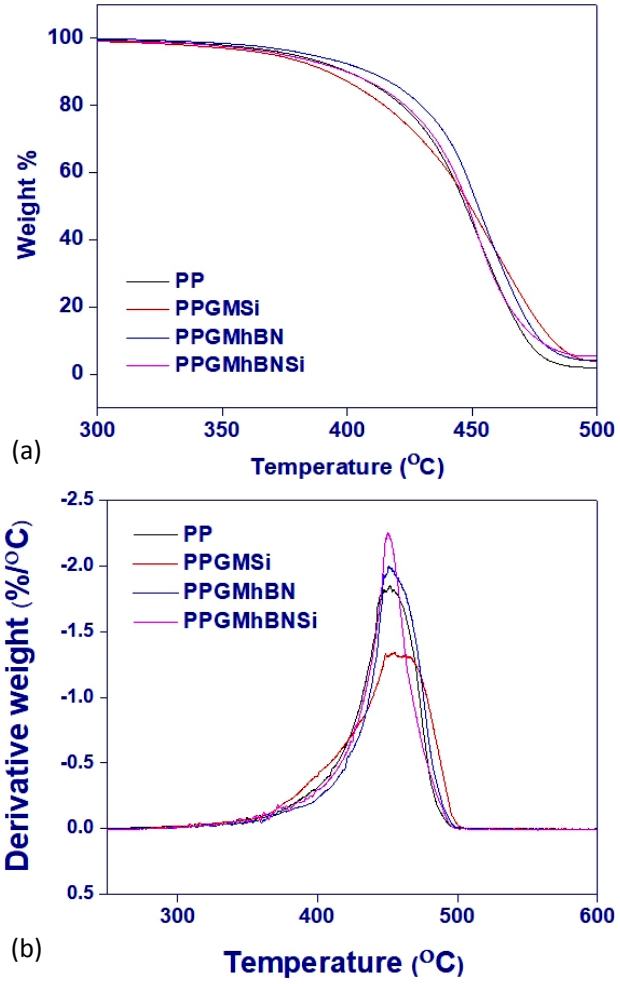

Figure 7. TGA characterisation of PP and PP-based nanocomposites: (a) TGA curves and (b) DTGA curves

SEM was carried out over the fractured samples to understand the mechanism of tensile deformation of PP and PP-based nanocomposites. Figure 9a shows the fracture surface of PP, showing the fibril formation and depicting the ductile fracture. Figure 9b shows the fracture surface of the PP/Si nanocomposite and the dispersion of aggregates of silica nanoparticles. Due to the aggregation of silica in the PP matrix, tensile properties decrease. Figure 9c shows the fracture surface of the PP/hBN nanocomposite, showing the formation of fibrils and shear bands and depicting the aggregated dispersion of h-BN nanosheets in the PP matrix. Due to the aggregation of h-BN nanosheets in the PP matrix, tensile properties decrease. Figure 9d shows the formation of fine fibrils in the PP/Si/hBN nanocomposite, depicting the finer dispersion of hybrid nanofillers. The finer dispersion of hybrid filler in the PP matrix exhibits a lesser amount of PP between fillers, which facilitates the formation of finer fibrils.

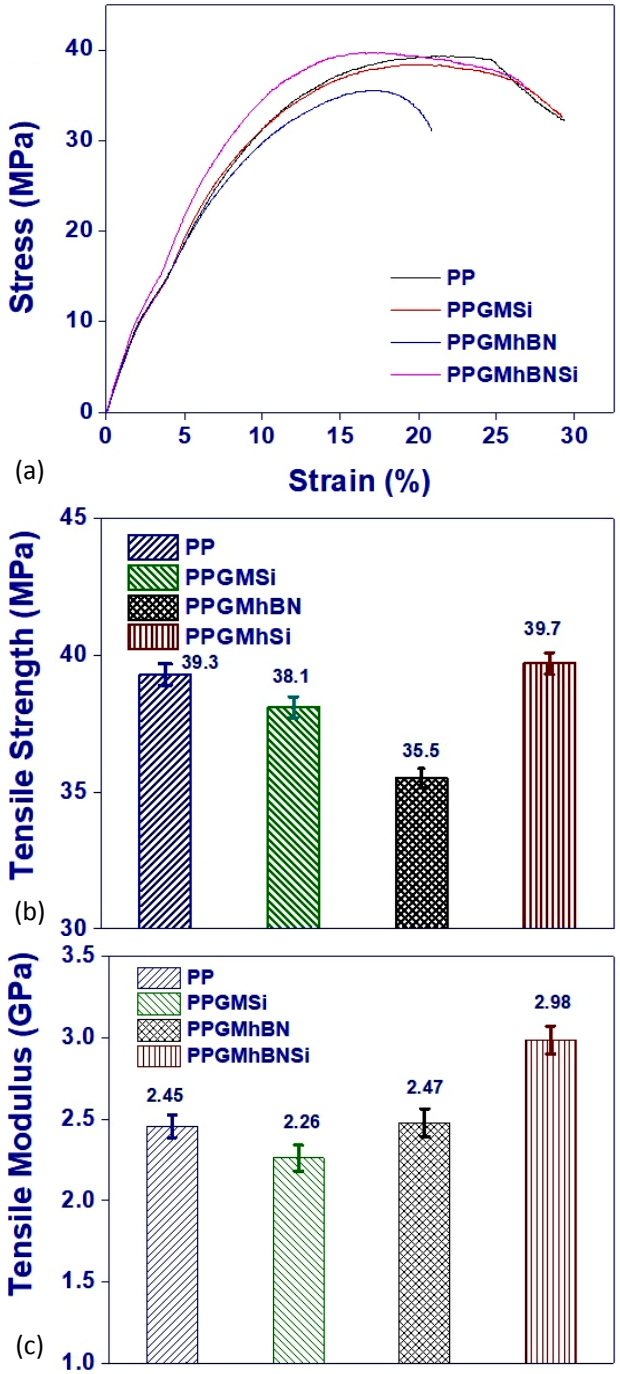

Figure 8. Tensile characterisation of PP and PP-based nanocomposites: (a) stress-strain curves, (b) tensile strength and (c) tensile modulus

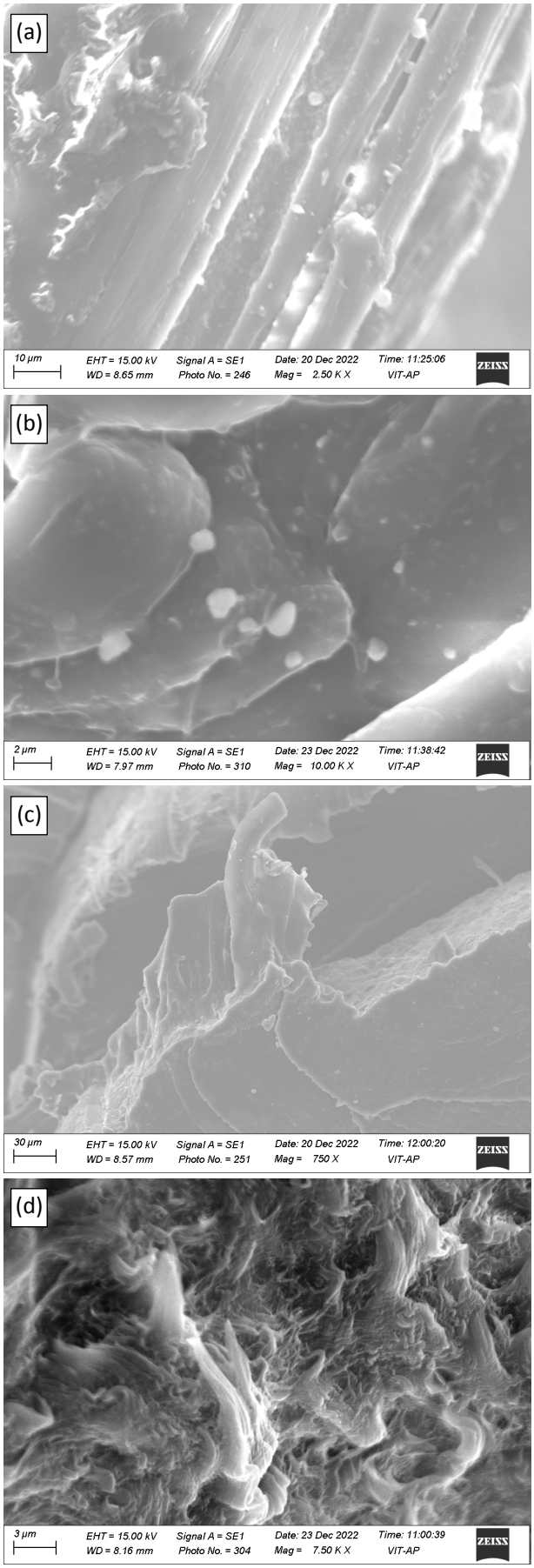

Figure 9. SEM images of PP and PP-based nanocomposites: (a) neat PP, (b) PP/Si, (c) PP/hBN and (d) PP/hBN/Si

It is important to note that the crystallinity of PP/Si/hBN nanocomposite is higher than that of neat PP. From rheological characterisation, the viscosity of PP/Si/hBN nanocomposite is higher than that of neat PP. Thus, the rheological, fracture and DSC characterisation depict the finer dispersion of h-BN nanosheets and silica nanoparticles in the PP matrix. Finer dispersion of h-BN nanosheets and silica nanoparticles in the PP matrix increases the crystallinity, viscosity and fine fibril formation, enhancing mechanical properties. Finer fibrils signify a higher load-bearing capacity.

3.8 Tribological characterisation

Tribological studies have been carried out over PP and PP-based nanocomposites. Figure 10 shows the wear as a function of time for the PP and PP-based nanocomposites. The wear of PP increases with time, depicting the running-in stage of wear when the thickness of the worn material increases. After 200 s of sliding, the wear reaches a steady state. After 144 s, there is an accelerated wear of PP due to fatigue. The addition of silica in PP shows a decrease in wear as compared to PP. This is due to the addition of hard silica nanoparticles resisting the wear. Fluctuations in PP/Si nanocomposite wear are noticed due to the precedence of hard silica abrasive particles. After 600 s, the PP/Si starts to wear significantly due to the layer of PP with silica nanoparticles deposited over the metal surface, acting as a hard abrasive.

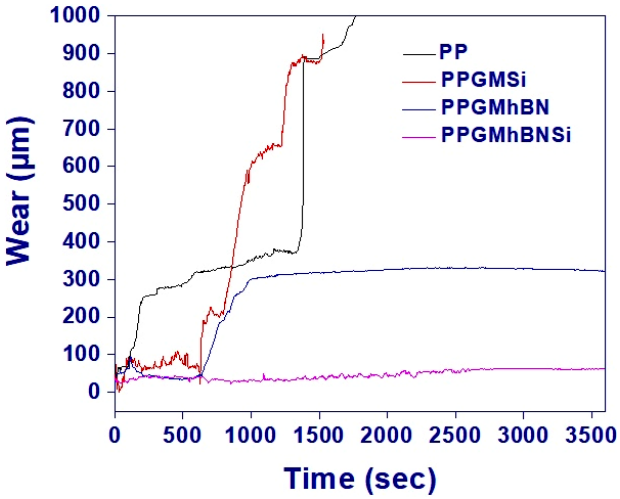

Figure 10. Wear vs. time for PP and PP-based nanocomposites

Adding h-BN nanosheets in PP decreases the wear as compared to PP and PP/Si nanocomposite for 600 s. This is due to the multilayer dispersion of h-BN nanosheets in the PP matrix, which are

mobile during deformation and resist wear. Thereafter a gradual increase in wear is noticed for PP/hBN nanocomposite up to 1000 s. After 1000 s, a steady-state wear of PP/hBN nanocomposite was noticed up to 3600 s, which depicts that the wear is due to the sliding of PP/hBN nanocomposite against the deposited layer of PP/hBN nanocomposite. The incorporation of silica nanoparticles and h-BN nanosheets in the PP matrix shows the lowest wear for 3600 s of testing. This reflects the synergistic effect of hybrid filler components on the wear resistance of PP.

To understand the steady-state wear of PP/hBN/Si and PP/hBN nanocomposites in detail, wear was closely analysed in Figure 11, which shows the wear results for a 1000 – 3600 s testing period. The long sliding distance wear studies can reveal insights into the adhesive wear of PP-based nanocomposites. After the formation of the PP-based nanocomposites layer, the appearance of the contacting surfaces is similar to the adhesive wear mechanism. During adhesive wear, material transfer and debris formation take place. For PP/hBN nanocomposite, the wear increases with time up to 2400 s, which depicts the transfer of material over the counter-body surface. The slope of wear with time for PP/hBN nanocomposite was calculated as 1.2 µm/min. After 2400 s, the measured worn material thickness of PP/hBN nanocomposite shows a decrease with time. This reflects the formation of wear debris, which contributes to the removal of PP/hBN nanocomposite from the counter-body surface.

The wear results for the 1000 – 2600 s range of PP/hBN/Si nanocomposite show an increase in wear, depicting the transfer of material from the sample to the counter-body metal disc. The slope of wear with time for PP/hBN/Si nanocomposite was calculated as 0.9 µm/min. After 2600 s, the wear is in the range from 60 to 64 µm for PP/hBN/Si nanocomposite, which is shown as detail image inserted in Figure 11. This depicts that the debris formation and materials transfer occur simultaneously. The important thing to note is that the hybrid filler dispersion in the PP matrix is fine, as depicted earlier in rheology, crystallinity, tensile and SEM studies. The finer dispersion of hybrid filler increases the interfacial contact between the nanofiller and PP, contributing to higher wear resistance.

Figure 12 shows the coefficient of friction (µ) as a function of time for the PP and PP-based nanocomposites. It was noted that the µ value increases with time for PP due to three-stage friction behaviour. The µ value for PP/Si nanocomposite is lower in comparison to PP. The µ value for PP/Si nanocomposite is steady-state from 600 s onwards. This is due to the wear debris of silica, acting as an abrasive. Hard silica nanoparticle debris easily wear the PP/Si nanocomposite, thus reducing the friction force.

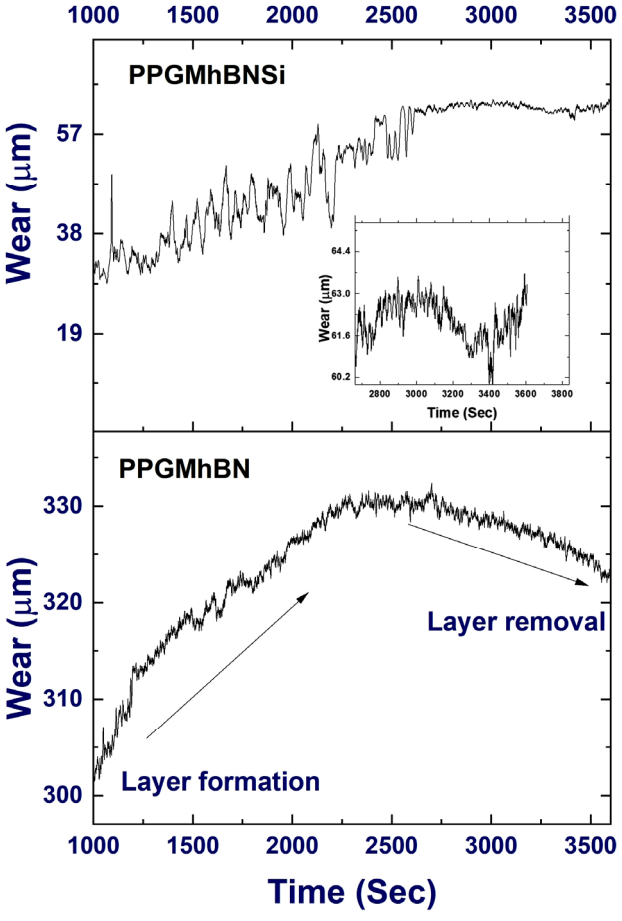

Figure 11. Wear vs. time for PP/hBN/Si and PP/hBN nanocomposites

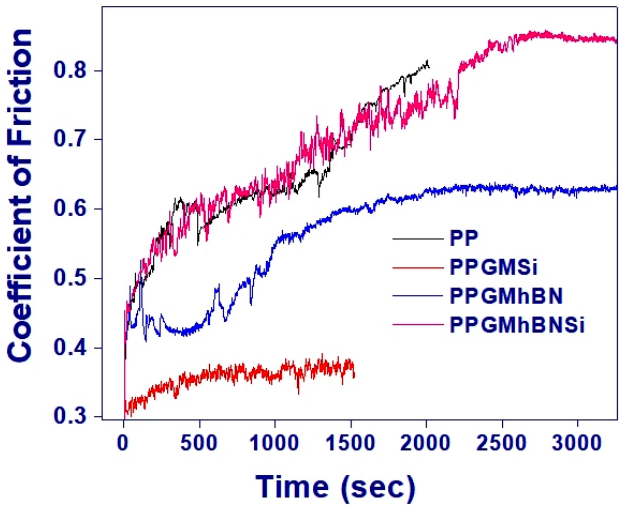

Figure 12. Coefficient of friction vs. time for PP and PP-based nanocomposites

Incorporating h-BN nanosheets in the PP matrix has shown an increase in μ value compared to PP/Si nanocomposite. The μ for PP/hBN nanocomposite reached steady-state after 1600 s. The higher μ for PP/hBN nanocomposite is because multilayered h-BN nanosheets debris undergoes slip which has to overcome higher shear forces at the interface, which increases frictional force. The μ for PP/hBN/Si nanocomposite is the highest among all PP-based nanocomposites. Since PP/hBN/Si nanocomposite has the lowest wear rate, debris accumulation is slower. The wear debris layer, once formed, needs a higher force for wear to occur due to the finer dispersion of hybrid filler in the PP matrix. The h-BN nanosheets protect from the abrasive action of silica nanoparticles, while silica facilitates the finer h-BN dispersion in the PP matrix, resulting in improved wear resistance. The average μ value in the steady-state range is 0.36 for PP/Si nanocomposite, 0.6 for PP/hBN nanocomposite and 0.85 for PP/hBN/Si nanocomposite.

4. Conclusions

The h-BN nanosheets were synthesised and characterised. The obtained h-BN nanosheets are multilayered.

Rheological characterisation suggests that the finer dispersion of hybrid fillers in the PP matrix is due to the highest increase in viscosity in the zero shear zone. Flow behaviour index values were less than 1, which depicts the pseudoplastic fluid behaviour for PP-based nanocomposites.

XRD observation reveals the formation of PP crystals in PP-based nanocomposites. The DSC characterisation reveals the increase in crystallinity and crystallisation temperature of PP-based nanocomposites, depicting the heterogeneous nucleating action of solid fillers on the PP matrix.

The tensile strength and tensile modulus of hybrid filler-reinforced PP-based nanocomposites increased by 1 and 25 %, respectively, due to the finer dispersion of hybrid fillers and the formation of finer fibrils as observed in fractography studies.

The hybrid filler-reinforced PP-based nanocomposites showed the lowest wear, reflecting the synergistic effect of hybrid components on the wear resistance of PP.

References

[1] P. Kubade, P. Tambe, Influence of surface modification of halloysite nanotubes and its localization in PP phase on mechanical and thermal properties of PP/ABS blends, Composite Interfaces, Vol. 24, No. 5, 2017, pp. 469-487, DOI: 10.1080/09276440.2016.1235442

[2] P.B. Tambe, A.R. Bhattacharyya, A.R. Kulkarni, The influence of melt-mixing process conditions on electrical conductivity of polypropylene/multiwall carbon nanotubes composites, Journal of Applied Polymer Science, Vol. 127, No. 2, 2013, pp. 1017-1026, DOI: 10.1002/app.37889

[3] P. Kubade, P. Tambe, Influence of halloysite nanotubes (HNTs) on morphology, crystallization, mechanical and thermal behaviour of PP/ABS blends and its composites in presence and absence of dual compatibilizer, Composite Interfaces, Vol. 23, No. 5, 2016, pp. 433-451, DOI: 10.1080/09276440.2016.1144392

[4] P.B. Tambe, A.R. Bhattacharyya, S.S. Kamath, A.R. Kulkarni, T.V. Sreekumar, A. Srivastav, K.U. Bhasker Rao, Y. Liu, S. Kumar, Structure-property relationship studies in amine functionalized multiwall carbon nanotubes filled polypropylene composite fiber, Polymer Engineering & Science, Vol. 52, No. 6, 2012, pp. 1183-1194, DOI: 10.1002/pen.22186

[5] G. Lohar, P. Tambe, B. Jogi, Influence of dual compatibilizer and carbon black on mechanical and thermal properties of PP/ABS blends and their composites, Composite Interfaces, Vol. No. 12, 2020, pp. 1101-1136, DOI: 10.1080/09276440.2020.1726137

[6] M. Tanniru, P. Tambe, Selective localization of rice husk derived graphene in reactive compatibilized PP/PA6 blends: Influence on morphology, interface and mechanical properties, Fullerenes, Nanotubes and Carbon Nanostructures, Vol. 30, No. 2, 2022, pp. 242-257, DOI: 10.1080/1536383X.2021.1929191

[7] B.C. Bal, N. Narlioğlu, Physical and mechanical properties of composites produced from recycled polypropylene and cardboard-polyethylene-aluminium mixture, Tribology and Materials, Vol. 3, No. 4, 2024, pp. 163-171, DOI: 10.46793/tribomat.2024.018

[8] R. Sinha, S. Sengupta, S. Jayapalan, Effect of hybrid fillers on the mechanical behavior of polypropylene based hybrid composites, Journal of the Indian Chemical Society, Vol. 99, No. 2, 2022, Paper 100317, DOI: 10.1016/j.jics.2021.100317

[9] M.G. Rasul, A. Kiziltas, B. Arfaei, R. Shahbazian-Yassar, 2D boron nitride nanosheets for polymer composite materials, npj 2D Materials and Applications, Vol. 5, 2021, Paper 56, DOI: 10.1038/s41699-021-00231-2

[10] L. Boldrin, F. Scarpa, R. Chowdhury, S. Adhikari, Effective mechanical properties of hexagonal

boron nitride nanosheets, Nanotechnology, Vol. 22, No. 50, 2011, Paper 505702, DOI: 10.1088/0957-4484/22/50/505702

[11] S. Kong, H. Seo, H. Shin, J.-H. Baik, J. Oh, Y.-O. Kim, J.-C. Lee, Improvement in mechanical and thermal properties of polypropylene nanocomposites using an extremely small amount of alkyl chain-grafted hexagonal boron nitride nanosheets, Polymer, Vol. 180, 2019, Paper 121714, DOI: 10.1016/j.polymer.2019.121714

[12] D.S. Muratov, V.O. Vanyushin, L.O. Luchnikov, M.Y. Degtyaryov, E.A. Kolesnikov, A.A. Stepashkin, D.V. Kuznetsov, Improved thermal conductivity of polypropylene filled with exfoliated hexagonal boron nitride (hBN) particles, Materials Research Express, Vol. 8, No. 3, 2021, Paper 035010, DOI: 10.1088/2053-1591/abed0f

[13] S. Meer, A. Kausar, T. Iqbal, Attributes of polymer and silica nanoparticle composites: A review, Polymer-Plastics Technology and Engineering, Vol. 55, No. 8, 2016, pp. 826-861, DOI: 10.1080/03602559.2015.1103267

[14] M. Kaseem, Z.U. Rehman, S. Hossain, A.K. Singh, B. Dikici, A review on synthesis, properties, and applications of polylactic acid/silica composites, Polymers, Vol. 13, No. 18, 2021, Paper 3036, DOI: 10.3390/polym13183036

[15] M. García, G. van Vliet, S. Jain, B.A.G. Schrauwen, A. Sarkissov, W.E. van Zyl, B. Boukamp, Polypropylene/SiO_2 nanocomposites with improved mechanical properties, Reviews on Advanced Materials Science, Vol. 6, No. 2, 2004, pp. 169-175.

[16] H. Palza, R. Vergara, P. Zapata, Composites of polypropylene melt blended with synthesized silica nanoparticles, Composites Science and Technology, Vol. 71, No. 4, 2011, pp. 535-540, DOI: 10.1016/j.compscitech.2011.01.002

[17] A. Kufel, S. Para, S. Kuciel, Basalt/glass fiber polypropylene hybrid composites: Mechanical properties at different temperatures and under cyclic loading and micromechanical modelling, Materials, Vol. 14, No. 19, 2021, Paper 5574, DOI: 10.3390/ma14195574

[18] A.K. Nurdina, M. Mariatti, P. Samayamutthirian, Effect of single-mineral filler and hybrid-mineral filler additives on the properties of polypropylene composites, Journal of Vinyl and Additive Technology, Vol. 15, No. 1, 2009, pp. 20-28, DOI: 10.1002/vnl.20173

[19] J. Hartikainen, P. Hine, J.S. Szabó, M. Lindner, T. Harmia, R.A. Duckett, K. Friedrich, Polypropylene hybrid composites reinforced with long glass fibres and particulate filler, Composites Science and Technology, Vol. 65, No. 2, 2005, pp. 257-267, DOI: 10.1016/j.compscitech.2004.07.010

[20] M.T. Hayajneh, F.M. Al-Oqla, M.M. Al-Shrida, Hybrid green organic/inorganic filler polypropylene composites: Morphological study and mechanical performance investigations, e-Polymers, Vol. 21, No. 1, 2021, pp. 710-721, DOI: 10.1515/epoly-2021-0074

[21] E. Watt, M.A. Abdelwahab, M.R. Snowdon, A.K. Mohanty, H. Khalil, M. Misra, Hybrid biocomposites from polypropylene, sustainable biocarbon and graphene nanoplatelets, Scientific Reports, Vol. 10, 2020, Paper 10714, DOI: 10.1038/s41598-020-66855-4

[22] N.D. Aparna, P. Tambe, Functionalized boron nitride nanosheets and their polypropylene nanocomposites: influence on thermal, mechanical, rheological and wear behaviour, Composite Interfaces, Vol. 31, No. 12, 2024, pp. 1415-1442, DOI: 10.1080/09276440.2024.2350170

[23] B.L.N. Krishna Sai, P. Tambe, Surface modified hollow glass microsphere reinforced 70/30 (wt/wt) P.C/A.B.S blends: Influence on rheological, mechanical, and thermo-mechanical properties, Composite Interfaces, Vol. 29, No. 6, 2022, pp. 617-641, DOI: 10.1080/09276440.2021.1986974